Journal of Visualized Experiments

Helical organization of blood coagulation Factor VIII on lipid nanotubes

--Manuscript Draft--

Manuscript Number:	JoVE51254R5
Full Title:	Helical organization of blood coagulation Factor VIII on lipid nanotubes
Article Type:	Invited Methods Article - JoVE Produced Video
Keywords:	Cryo-electron microscopy, Lipid nanotubes, Helical assembly, Membrane-bound organization, Coagulation factor VIII,
Manuscript Classifications:	1.7: Cardiovascular System; 3.14.907: Vascular Diseases; 4.10.570: Membrane Lipids; 4.10.808: Sphingolipids; 95.51.24: life sciences; 95.51.6: biochemistry; 95.51.8: bioengineering (general)
Corresponding Author:	Svetla Stoilova-McPhie, Ph.D. University of Texas Medical Branch Galveston, Texas UNITED STATES
Corresponding Author Secondary Information:	
Corresponding Author E-Mail:	svmcphie@utmb.edu
Corresponding Author's Institution:	University of Texas Medical Branch
Corresponding Author's Secondary Institution:	
First Author:	Jaimy L Miller, BSC
First Author Secondary Information:	
Other Authors:	Jaimy L Miller, BSC
	Daniela Dalm
	Alexey Y Koyfman
	Kirill Grushin
Order of Authors Secondary Information:	
Abstract:	Cryo-electron microscopy (Cryo-EM)1 is a powerful approach to investigate the functional structure of proteins and complexes in a hydrated state and membrane environment 2. Coagulation Factor VIII (FVIII)3 is a multi-domain blood plasma glycoprotein. Defect or deficiency of FVIII is the cause for Hemophilia type A - a severe bleeding disorder. Upon proteolytic activation, FVIII binds to the serine protease Factor IXa on the negatively charged platelet membrane, which is critical for normal blood clotting4. Despite the pivotal role FVIII plays in coagulation, structural information for its membrane-bound state is incomplete5. Recombinant FVIII concentrate is the most effective drug against Hemophilia type A and commercially available FVIII can be expressed as human or porcine, both forming functional complexes with human Factor IXa 6,7. In this study we present a combination of Cryo-electron microscopy (Cryo-EM), lipid nanotechnology and structure analysis applied to resolve the membrane-bound structure of two highly homologous FVIII forms: human and porcine. The methodology developed in our laboratory to helically organize on negatively charged lipid nanotubes (LNT) the two functional recombinant FVIII forms is described. The representative results demonstrate that our approach is sufficiently sensitive to define the differences in the helical organization between the two highly homologous in sequence (86% sequence identity) proteins. Detailed protocols for the helical organization, Cryo-EM and electron tomography (ET) data acquisition are given. The two-dimensional (2D) and three-dimensional (3D) structure analysis applied to obtain the 3D reconstructions of human and porcine FVIII-LNT is discussed. The presented human and porcine FVIII-

	LNT structures show the potential of the proposed methodology to calculate the functional, membrane-bound organization of blood coagulation Factor VIII at high resolution.
Author Comments:	Dear Dr. Cherny, Please find enclosed a list of changes, where we respond top each of the editorial comments individually, marked with (#). Editorial comments: *Please use track changes in Microsoft word when making revisions. #We have used the "Track-changes" options in Microsoft word when making the revisions. *The abstract is not suitable for an introduction. #We have added an introduction section. ** Please write an introduction that covers in at least two paragraphs: 1) A clear statement of the overall goal of this method, 2) the rationale behind the development and/or use of this technique, 3) the advantages over alternative techniques with applicable references to previous studies where the technique was used, 4) a description of the context of the technique in the wider body of literature, and 5) information that can help readers determine if the method described is appropriate for their application. #We have added an introduction section covering four paragraphs addressing the goal, rationale, context of the technique and advantages of the proposed method. *There must be a single space between each step of the protocol including headers. #We have added single space between each step in the PROTOCOL. * Please highlight in yellow using the highlight tool the sections of your protocol that you wish to film. Note you can only highlight up to 2.75 pages of protocol text. Please refer to the authors instructions on the JoVE website for additional details. We have highlighted the sections of the protocol to be filmed. We have left the subtitles: MOVIE 1, 2, 3. * Please read protocol steps for clarity/copyediting. (2.2.1, 2.2.2, etc...) ** Please note: many steps are unclear #We have read and clarified the steps of the protocol. *** Subset of examples: Steps 3.2.2-4.25. How are these accomplished, are these computation steps? Does this require running scripts? Please describe in enough detail that a first time user could perform these actions. Note: not the only examples. #We have added additional information. All documentation for the EMAN2 algorithms used in out methodology is given in details on the EMAN2 documentation website, for which we have included the link in the text. We have given the script we use for the 2D classification. For most of the steps we use GUI, for which the instruction are given on the EMAN2 documentation website. We have also provided the specific links for each EMAN2 option used in the protocol. * Text under step 3 needs to be preceded by a Note. #We have clarified the text under step 3. * Numbering is incorrect starting at 3.3 #We have corrected the numbering.

	* Please ensure that all appropriate images are presented with scale bars. #Where there are no scale bars on the images, the pixel size and dimensions of the structures are given in the figure legend. These values are more accurate and often used as an alternative of a scale bar in structural Cryo-electron microscopy. *JoVE is unable to publish manuscripts containing commercial sounding language, including the mention of company brand names before an instrument or reagent. #We have removed commercially sounding language. ** In instances where the use of a specific type of material or equipment will directly affect the protocol outcome or parameters you may use the specific name when you introduce the equipment and then refer to it by more generic terms thereafter. * Please include DOI numbers for your reference section as follows: [Lastname, F.I., LastName, F.I., LastName, F.I. Article Title. Source. Volume (Issue), FirstPage - LastPage, doi:DOI, (YEAR).] #We have reformatted according to the JoVE endnote format. Some references do not have a DOI number when this format is applied.
Additional Information:	
Question	**Response**

utmb Health

SCHOOL OF MEDICINE

DEPARTMENT OF NEUROSCIENCE AND CELL BIOLOGY

To the Editor of JoVE
att, Dr. Rachelle Baker, Associate Editor

June 3rd, 2013

Dear Sir.Madam,

I would like to submit our manuscript entitled: "**Helical organization of blood coagulation Factor VIII on lipid nanotubes**", as an invited methods article with JoVE produced video.

In this work we are presenting the methodology developed in our laboratory to helically organize membrane-bound coagulation proteins on single bilayer lipid nanotubes, at close to physiological conditions. By combining Cryo-electron microscopy with engineered protein-lipid helical assembly and structure analysis, we are able to resolve the membrane-bound structure of clinically important proteins as coagulation Factor VIII.

Developing further the presented approach will have a significant implication for the field of structure determination of membrane an membrane-associated proteins at close to physiological conditions, which will help identify the protein-protein and protein-membrane interface critical for their function.

Sincerely,

Svetla S. McPhie

Svetla Stoilova-McPhie. PhD
Assistant Professor
Neuroscience and cell Biology
Sealy Centre for Structural Biology and Molecular Biophysics
University of Texas Medical Branch, Galveston, TX, 77555, USA

Helical organization of blood coagulation Factor VIII on lipid nanotubes.

Jaimy Miller[†‡], Daniela Dalm[†‡], Alexey Y. Koyfman[#,§], Kirill Grushin[†] and Svetla Stoilova-McPhie [†,§*]

[†]Department of Neuroscience and Cell Biology, [#]Department of Biochemistry and Molecular Biology and [§]Sealy Center for Structural Biology and Molecular Biophysics, University of Texas Medical Branch, Galveston, TX, 77555, USA.

*Corresponding author, Tel: +1-979-319-1349; fax: +1-409-747-2200. E-mail address: svmcphie@utmb.edu
[‡]equal contribution

KEYWORDS
Cryo-electron microscopy, Lipid nanotubes, Helical assembly, Membrane-bound organization, Coagulation factor VIII,

SHORT ABSTRACT
We present a combination of Cryo-electron microscopy, lipid nanotechnology and structure analysis applied to resolve the membrane-bound structure of two highly homologous FVIII forms: human and porcine. The methodology developed in our laboratory to helically organize on negatively charged lipid nanotubes (LNT) the two functional recombinant FVIII forms is described.

ABSTRACT
Cryo-electron microscopy (Cryo-EM)[1] is a powerful approach to investigate the functional structure of proteins and complexes in a hydrated state and membrane environment [2].

Coagulation Factor VIII (FVIII)[3] is a multi-domain blood plasma glycoprotein. Defect or deficiency of FVIII is the cause for Hemophilia type A - a severe bleeding disorder. Upon proteolytic activation, FVIII binds to the serine protease Factor IXa on the negatively charged platelet membrane, which is critical for normal blood clotting[4]. Despite the pivotal role FVIII plays in coagulation, structural information for its membrane-bound state is incomplete[5]. Recombinant FVIII concentrate is the most effective drug against Hemophilia type A and commercially available FVIII can be expressed as human or porcine, both forming functional complexes with human Factor IXa [6,7].

In this study we present a combination of Cryo-electron microscopy (Cryo-EM), lipid nanotechnology and structure analysis applied to resolve the membrane-bound structure of two highly homologous FVIII forms: human and porcine. The methodology developed in our laboratory to helically organize on negatively charged lipid nanotubes (LNT) the two functional recombinant FVIII forms is described. The representative results demonstrate that our approach is sufficiently sensitive to define the differences in the helical organization between the two highly homologous in sequence (86%

sequence identity) proteins. Detailed protocols for the helical organization, Cryo-EM and electron tomography (ET) data acquisition are given. The two-dimensional (2D) and three-dimensional (3D) structure analysis applied to obtain the 3D reconstructions of human and porcine FVIII-LNT is discussed. The presented human and porcine FVIII-LNT structures show the potential of the proposed methodology to calculate the functional, membrane-bound organization of blood coagulation Factor VIII at high resolution.

INTRODUCTION

Blood coagulation Factor VIII (FVIII) is a large glycoprotein of 2332 amino acids organized in six domains: A1-A2-B-A3-C1-C2 [3]. Upon Thrombin activation FVIII acts as the co-factor to Factor IXa within the membrane-bound Tenase complex. Binding of activated FVIII (FVIIIa) to FIXa in a membrane-depending manner enhances FIXa proteolytic efficiency more than 10^5 times, which is critical for efficient blood coagulation [4]. Despite the important role FVIII plays in coagulation and the Tenase complex formation, the functional membrane-bound FVIII structure is yet to be resolved.

To address this, single lipid bilayer nanotubes (LNT) rich in phosphatidylserine (PS), capable of binding FVIII with high affinity [8,9] and resembling the activated platelet surface have been developed [10]. Consecutive helical organization of FVIII bound to LNT has been proven to be effective for structure determination of FVIII membrane-bound state by Cryo-EM [5]. Functionalized LNT are an ideal system to study protein-protein and protein-membrane interactions of helically organized membrane-associated proteins by Cryo-EM [11,12]. Cryo-EM has the advantage over traditional structural methods as X ray crystallography and NMR, as the specimen is preserved at closest to the physiological environment (buffer, membrane, pH), without additives and isotopes. In the case of FVIII, studying the membrane-bound structure with this technique is even more physiologically relevant, as the LNT resemble closely by size, shape and composition the pseudopodia of the activated platelets where the Tenase complexes assemble *in vivo*.

Defects and deficiency of FVIII cause Hemophilia A, a severe bleeding disorder affecting 1 in 5,000 males of the human population [4,6]. The most effective therapy for Hemophilia A is life-long administration of recombinant human FVIII (hFVIII). A significant complication of the recombinant FVIII Hemophilia A therapy is the development of inhibitory antibodies to the human form affecting approximately 30% of Hemophilia A patients [13]. In this case, porcine FVIII (pFVIII) concentrate is used, as porcine FVIII displays low cross-reactivity with inhibitory antibodies against human FVIII and forms functional complexes with human FIXa [7]. Establishing the membrane-bound organization of both porcine and human FVIII forms is important to understand the structural basis of FVIII cofactor function and implications for blood hemostasis.

In this study, we describe a combination of lipid nanotechnology, Cryo-EM, and structure analysis designed to resolve the membrane-bound organization of two highly homologous FVIII forms. The presented Cryo-EM data and 3D structures for helically organized porcine and human FVIII on negatively charged LNT show the potential of the

proposed nanotechnology as basis for structure determination of FVIII and membrane-bound coagulation factors and complexes in a physiological membrane environment.

PROTOCOL

1. Sample preparation.

1.1. Buffer exchange human FVIII-BDD[14] and porcine FVIII-BDD[15] against HBS-Ca buffer (20 mM HEPES, 150 mM NaCL, 5 mM $CaCl_2$, pH=7.4) and concentrate to 1.2 mg/ml. Keep the protein solution at -80 ^{o}C.

1.2. Prepare lipid nanotubes (LNT) by mixing GalactosylCeramide (GC) and phosphatidylserine (PS) at 1:4 w/w ratio in chloroform. Evaporate the chloroform under argon and solubilize the lipids in HBS buffer to 1mg/ml. Keep the LNT solution at 4 ^{o}C.

2. Cryo-electron microscopy of FVIII-LNT.

2.1. Cryo-EM sample preparation.

2.1.1. Glow discharge the 300 mesh Quantifoil R2/2 copper grids (carbon side up) in a mixture of O_2 and He gas for 10 seconds at 50 W.

2.1.2. Mix the FVIII and LNT solutions in HBS-Ca buffer at 1:1 w/w ratio and incubate for 15 minutes at room temperature.

2.1.3. Apply a drop of 2.5 µl of FVIII-LNT sample to the hydrophilic electron microscopy grid in the Vitrobot Mark IV humidified chamber (100% humidity).

2.1.4. Blot and flash freeze the grid (one blot for 3.5 seconds, blot force 1) in liquid C_2H_6, cooled down by liquid N_2 to obtain amorphous ice.

2.1.5. Store grids in storage boxes under liquid N_2 (LN2).

2.2. Cryo-EM data collection

NOTE: The JEM2100-LaB6 (year 2010) is equipped with a TEMCON operating system consisting of a computer connected to the electron microscope, a screen with windows reading the vacuum system, illumination system, HT, lens currents and so-on, and two panels: LEFT and RIGHT, placed on both side of the column. The beam shift X,Y knobs (SHIFT Y, SIFT Y) and the multifunction (DEF/STIG) knobs are on both panels. On the LEFT panel is the illumination (BRIGTHNESS) knob. On the RIGHT panel are: the magnification (MAG/CAM LENGTH) and focus (FOCUS) knobs and the three imaging (MAG1, MAG2, LOWMAG) and a diffraction (DIFF) modes buttons. We acquire our data in MAG1 at alpha 2. The minimum dose illumination conditions (MDS) required for Cryo-EM data acquisition are set with F1 through F6 buttons, top row on RIGHT panel. In this protocol the generic settings are used: F1 - raise/lower screen, F2 - SEARCH

mode, F3 – FOCUS mode, F4 – PHOTO mode, F5 – MDS OFF/ON and F6 – BEAM BLANK, used to shield the specimen from radiation damage by deflecting the beam.

2.2.1. Place the cryo-holder into the cryo-station and fill the Dewar of the holder and the cryo-station with LN2. When temperature reaches -192 ^{o}C, open shutter on the holder tip, place previously frozen Cryo-EM grid into the designated place and secure with a ring clamp.

2.2.2. Insert the cryo-holder into the electron microscope. Refill the Dewar of the cryo-holder and the anti-contaminator chamber with LN2. Wait for the holder to stabilize for 30 – 60 minutes. Press F6 on and turn the filament on. When the filament is saturated, press F6 off and open shutter on holder to view the grid.

2.2.3. Press LOW MAG / alpha 1 (set at 200x mag) and locate areas with thin ice on the grid.

2.2.4. Switch to MAG 1 / alpha 2 to set minimum dose (MDS) mode and acquire Cryo-EM data at low electron doses, without damaging the specimen.

2.2.4.1. Press F2 to set SEARCH MODE. Set magnification at 40,000x. Enlarge beam with BRIGTNESS knob to minimal electron dose ~ 0.04 $e^{-}/Å^{2}$*s. Press DIFF to switch to diffraction mode. Set camera length to 120cm with MAG/CAM LENGHT knob. Locate areas on the grid within the pre-selected areas in LOWMAG that have lipid nanotubes in the holes of the carbon film.

2.2.4.2. Press F4 to set PHOTO mode at 40,000x magnification and set illumination with BRIGHTNESS knob at doses of 16-25 $e^{-}/Å^{2}$*s. Press STANDARD FOCUS button to set focus conditions adjusting the Z-height of the specimen with the Z UP/DOWN buttons (RIGHT control panel). Set defocus between -1.5 and -2.5 µm.

2.2.4.3. Align SEARCH and PHOTO mode by drawing a square in the LIVE VIEW window on the digital camera monitor in SEARCH mode corresponding to the area to be imaged in PHOTO mode.

2.2.4.4. Press F3 to set FOCUS MODE at 100,000x magnification. Focus illumination to cover the CCD chip (~4 - 5 cm radius) and off axis to not irradiate the area to be imaged in PHOTO mode. Adjust defocus to ~ -1.5 and -2.5 µm with the FOCUS knob and correct for astigmatism of the image with DEF/STIG knobs.

2.2.5. Select the FVIII-LNT to be imaged in SEARCH mode by acquiring live images in the LIVE VIEW window on the digital camera monitor. Center the FVIII-LNT in the square drawn on the LIVE VIEW window.

2.2.6. Record a digital image on the CCD camera at 52,000x effective magnification and 0.5 s exposure by switching to PHOTO mode and clicking the ACQUIRE button on

the digital micrograph camera monitor. The image acquisition conditions are set such as the beam blank (SHUTTERS) open only when the image is acquired in PHOTO mode.

2.2.7. Check the quality and defocus of the acquired image by pressing CTRL-F to obtain a Fast Fourier Transform (FFT).

3. 3D reconstruction

NOTE: The image analysis software used for the 2D and 3D analysis: EMAN2 and IHRSR are freely available. EMAN2 can be downloaded from http://blake.bcm.edu/emanwiki/EMAN2/Install. The IHRSR software can be obtained from Professor Egelman: egelman@virginia.edu. The final IHRSR refinements are run on the Texas advanced computing center cluster: http://www.tacc.utexas.edu/ at the University of Texas, Austin. The 3D reconstruction algorithm shown on **Figure 1** consists of two main steps: First selecting a homogenous set of helical segments (particles) with the 2D reference free alignment (RFA) algorithms implemented in EMAN 2, second achieving a 3D reconstruction based on the helical parameters and back projection algorithms incorporated in IHRSR. The first step utilizes the programs developed for selecting homogenous particle sets for 3D reconstruction with Single Particle SPA (algorithms) for which EMAN2 has been specifically developed and distributed: http://blake.bcm.edu/emanwiki/EMAN2. This step has been adapted to the Cryo-EM data. The second step is achieved with the IHRSR algorithm, which is specifically designed for the type of helical assemblies obtained with the recombinant Factor VIII forms. This algorithm has been documented extensively through the scientific literature and specifically[12].

3.1. Perform 2D image analysis with the EMAN2 scientific image processing suite: http://blake.bcm.edu/eman2/doxygen_html/[16] to select homogenous particle (helical segment) sets for helical reconstruction.

3.1.1. Select Cryo-EM micrographs with straight and well organized helical tubes with the digital camera software and visualization tools.

3.1.2. Invert, normalize and filter for X-ray pixels in the *e2workflow.py* GUI, single particle reconstruction (SPR) option:
http://blake.bcm.edu/emanwiki/EMAN2/Programs/e2projectmanager

3.1.3. Import the inverted, normalized and X ray pixel filtered images in the *e2helixboxer.py* GUI. Select FVIII-LNT helical tubes and segment at 256x256 pixels (2.9 Å/pix) with 90% overlap using:
http://blake.bcm.edu/emanwiki/EMAN2/Programs/e2helixboxer

3.1.4 Evaluate the defocus from the original micrographs and apply contrast transfer function (CTF) correction (only phase correction) to the helical segments from the same micrographs with the *e2ctf.py* option incorporated in the *e2workflow.py*:
http://blake.bcm.edu/emanwiki/EMAN2/Programs/e2ctf.

3.1.5. Generate initial particles (helical segments) sets in the e2workflow.py GUI - SPR option: http://blake.bcm.edu/emanwiki/EMAN2/Programs/e2workflow.

3.1.6. Calculate 2D class averages with the e2refine2d.py algorithm applying reference free k-mean classification to select homogenous data sets with the same diameter LNT and degree of helical order (**Fig. 2**), following the script: 'e2refine2d.py --iter=8 --naliref=5 --nbasisfp=8 --path=r2d_001 --input=INPUT.hdf --ncls=51 --simcmp=dot --simalign=rotate_translate_flip --classaligncmp=dot --classraligncmp=phase --classiter=2 --classkeep=0.8 --classnormproc=normalize.edgemean --classaverager=mean --normproj –classkeepsig', changing the ncls value accordingly.

3.1.6.1. Classify the initial data set in 150 classes 'ncls=151' over 8 iterations with 'classkeep=0.8', meaning that particles with less than 80% similarity to the class average are excluded from the given class.
http://blake.bcm.edu/emanwiki/EMAN2/Programs/e2refine2d

3.1.6.2. Merge particles from class averages with pronounced helical diffraction in *e2display.py* to create intermediate data set.

3.1.6.3 Classify the intermediate data set in 50 classes 'ncls=51' to differentiate classes with same diameter and degree of order.

3.1.6.4. Merge particles from classes with same diameter and degree of order in *e2display.py* to create the final data set for the three-dimensional reconstruction: http://blake.bcm.edu/emanwiki/EMAN2/Programs/emselector.

3.2. Perform helical reconstruction with the Iterative Helical Real Space Reconstruction (IHRSR) algorithm, as described in [17,18].

3.2.1. Estimate the rise, Δz (Å) of the FVIII-LNT helix from the combined Fourier transform of the particles in the final data set.

3.2.2. Define the azimuthal angle $\Delta\phi$ (º) by running parallel IHRSR refinements with a constant Δz, increasing $\Delta\phi$ from 5^o to 60^o in 5^o increments.

3.2.3. Run 100 consecutive IHRSR cycles for each final data set with a featureless cylinder as an initial volume and the initial helical parameters Δz and $\Delta\phi$ as defined in 3.2.1. and 3.2.2.

3.2.4. Inspect the final volumes for convergence of the helical parameters and correspondence between class averages from the 2D classification of the final data set and the projections from the final IHRSR reconstruction.

3.2.5. Impose symmetry to the final 3D reconstructions, corresponding to the asymmetric unit distribution observed in the final asymmetric 3D volumes: 4-fold for the

human FVIII-LNT and 5-fold for the porcine FVIII-LNT. Run another 100 refinement cycles to generate a final symmetrized 3D reconstruction.

3.2.6. Calculate the Fourier Shell Correlation curve for both volumes by first separating the corresponding data set in odd and even: 'e2proc2d.py <infile> <outfile> --split=2'. Then run 100 IHRSR consecutive refinements as described in 3.2.3. Calculate the FSC of the 3D volumes created from the odd and even datasets: 'e2proc3d.py evenvolume.mrc fsc.txt --calcfsc=oddmap.mrc'.

3.3. Visualize and Segment the FVIII-LNT volumes in UCSF chimera**.**

3.3.1. Open the final volumes from step 3.2.5. in UCSF Chimera and set the contour level to 0.005 in the TOOLS > VOLUME DATA > VOLUME VIEWER option.

3.3.2. In TOOLS > VOLUME DATA > SEGMENT MAP, select volume in SEGMENT MAP tab and click on SEGMENT to segment the volume.

3.3.4. Group segments corresponding to one unit cell by selecting with CTRL+SHIFT and clicking group.

3.3.5. Color the segments by unit cell and helix with ACTIONS > COLOR option to emphasize the structural features.

4. Electron tomography.

4.1. Negatively stained FVIII-LNT sample preparation.

4.1.1. Prepare FVIII-LNT samples as for the Cryo-EM experiments.

4.1.2. Glow discharges carbon-coated 300-mesh copper grid (carbon side up) in a mixture of O_2 and He gas for 10 seconds at 50 W as for Cryo-EM experiments.

4.1.3. Apply a drop of 2.5 µl FVIII-LNT suspension with 6 nm colloidal gold nanoparticles to the grid, blot the excess liquid and negatively stain by applying 5 µl 1% Uranyl acetate solution for two minutes. Blot the excess liquid and air dry the grid.

4.2. Electron tomography data collection.

4.2.1. Transfer the grid into the single tilt holder.

4.2.2. Transfer the holder in the electron microscope.

4.2.3. Collect tilt series automatically with the SerialEM software[19] at 2° increments over an angular range of –60° to +60° and record images with a CCD camera at 52,000x effective magnification, -6 to -10 µm defocus and electron dose of 150 - 170 electrons/$Å^2$*s per tomogram.

4.3. Electron tomography reconstruction of FVIII-LNT.

Note: Reconstruct the pFVIII-LNT and hFVIII-LNT tilted series acquired in 4.2. with the ETomo option of the IMOD software following the tutorial: http://bio3d.colorado.edu/imod/doc/etomoTutorial.html

4.3.1. Using a terminal window, open the tomogram in 3DMOD. http://bio3d.colorado.edu/imod/doc/3dmodguide.html.

4.3.2. Bin the tomogram by 4 with the IMOD BINVOL command to decrease the size of the tomogram.

4.3.3. Select the proper angle to rotate the lipid nanotube along the Y axis in the binned tomogram using the IMOD ROTATEVOL command.

4.3.4. Rotate the full tomogram with the IMOD ROTATEVOL command.

4.3.5. Crop the selected lipid nanotube oriented along the Y axis with the IMOD CLIP RESIZE command.

4.3.6. Open the cropped sub-tomogram with 3DMOD.

4.3.7. Click on the tomogram to visualize the arrangement of Factor VIII molecules along the slices in Z axis and along Y axis in the sub-tomogram volume.

REPRESENTATIVE RESULTS

Recombinant human and porcine FVIII were successfully organized helically on negatively charged single bilayer LNT, resembling the activated platelet surface**.** The helical organization of the human and porcine FVIII-LNT was consistent through the collected digital micrographs (**Fig. 2)**. The control LNT and the human and porcine FVIII-LNT helical tubes were selected and segmented with the e2helixboxer.py GUI and initial data sets created with the e2workflow.py GUI, Single particle option (**Table 1**).

The helical order of the membrane-bound human and porcine FVIII-LNT was evaluated from the Fourier transform of the class averages with the e2display.py GUI (EMAN2) (**Fig. 3**). The lipid bilayer in the best control LNT 2D class averages is well defined. The inner and outer leaflet and lower density of the membrane hydrophobic core are clearly visible (**Fig. 3A**). The projected density of the membrane-bound human and porcine FVIII molecules oriented towards and perpendicular to the membrane surface is well defined and clearly shows the variations in the helical organization between the two proteins (**Fig. 3B,C**). The more pronounced twist for the human FVIII-LNT helical tubes indicates that the protein-protein interactions between adjacent membrane-bound FVIII molecules are consistently different for the two FVIII forms (**Fig. 3B,C**). Particles from class averages showing good helical organization (helical diffraction pattern) were merged in the e2display.py GUI to form an intermediate particle set (**Table 1**). The

particles from the intermediate particle sets were again classified in 50 classes with the same constraints. The particles from class averages with the same diameter were merged in the final data sets (**Table 1**).

Initial 3D reconstructions for the human and porcine FVIII-LNT were carried out with 1000 representative particles from the final human and porcine FVIII-LNT data sets. One hundred consecutive IHRSR iterations were run for each 3D reconstruction with a featureless cylinder (160 Å inner and 500 Å outer diameter), as initial volume. The axial rise (Δz) calculated from the combined Fourier transform of the helical segments (particles set) is equal to 41 Å for human FVIII-LNT and 36 Å for porcine FVIII-LNT (**Fig. 4A,B**). The initial azimuthal angle ($\Delta\phi$) defined from the iterative search is estimated at 40.0º for the human FVIII-LNT and at 35.0º for the porcine FVIII-LNT. The final volumes are inspected for convergence of the helical parameters and correspondence between class averages and projections from the final reconstruction, also following the criteria described in[5]. The selected 3D reconstructions and corresponding helical parameters are imposed as initial volumes and initial helical parameters for a second IHRSR refinement of 100 cycles which converged to a four-start helical organization for the human FVIII-LNT with Δz = 41.1 Å and $\Delta\phi$= 42.0 º and a five-start helical organization for the porcine FVIII-LNT with Δz = 35.5 Å and $\Delta\phi$= 34.8 º. A final 100 IHRSR iterations imposing a 4-fold and a 5-fold helical symmetry for the human and porcine FVIII-LNT reconstructions respectively are carried out with initial volumes and corresponding helical parameters from the last asymmetric IHRSR refinements (**Fig. 4C,D**). The final volumes show 8 human FVIII and 10 porcine FVIII membrane-bound molecules organized around the helical axis (**Fig. 5A)**. Each human FVIII molecule is translated 41.2 Å and rotated 42.0 º from the previous one and each porcine FVIII molecule is translated 35.9 Å and rotated 35.2 º from the previous one, corresponding to the helical parameters of the final 3D reconstructions (**Fig. 5B**).

The reconstructed electron tomograms confirm the difference in the helical organization between the human and porcine FVIII-LNT obtained at the same experimental conditions. Comparison of the top views from the reconstructed tomograms and the 3D volumes from the helical reconstruction viewed in the direction perpendicular to the helical axis, further validates the correctness of the 3D reconstructions refined with the IHRSR helical parameters (**Fig. 6**). The asymmetric 2D unit cell dimensions for the human FVIII-LNT 3D reconstruction are: a = 17.8 nm, b = 8.2, γ = 84 º and for the porcine FVIII-LNT 3D reconstruction: a = 18.4, b=7.2 and γ = 70 º (**Fig. 6**). The unit cell dimensions of human FVIII organized in membrane-bound 2D crystals are: a = 8.1, b=7.0 and γ = 67 º, which corresponds to the surface covered by one FVIII molecule viewed toward the membrane-surface[20]. Comparing the unit cell dimensions between FVIII organized in 2D and helical crystals indicates that both human and porcine FVIII molecules form dimers when helically organized on the LNT surface.

FIGURE CAPTIONS

Figure 1. Structure analysis flow chart. The steps followed for the 2D classification analysis based on reference free alignment algorithms implemented in EMAN2 [16] are circled in blue. The steps followed for the 3D analysis carried out with the iterative

helical real space reconstruction algorithms (IHRSR) are circled in red. The iterative IHRSR cycles are denoted with dashed arrows.

Figure 2. Cryo-EM digital micrographs (4096 x 4096 pixels, 2.9 Å/pix) of lipid nanotubes (LNT) with and without bound FVIII. A. Control LNT. B. Human FVIII-LNT. C. Porcine FVIII-LNT. The edge of the hole in the carbon film in which the FVIII-LNT are suspended in amorphous ice is indicated with a white star. The protein and lipid densities are in black. The magnified views (insets) of 512x512 cropped areas (white dashed square) illustrate the difference in the helical organization of the human and porcine FVIII, respectively. The scale bar is 100 nm.

Figure 3. Representative 2D class averages (top row) and corresponding Fourier transforms (bottom row) from the intermediate particle sets (**Table 1**) **classified in 50 classes**. **A. Control LNT B. Human FVIII-LNT C. Porcine FVIII-LNT**. The class number and number of particles included in each class are indicated. The difference in helical order between the human and porcine FVIII is clearly seen on the images and confirmed by the diffraction patterns obtained from the Fourier transforms of these images.

Figure 4. **3D helical reconstructions of human and porcine FVIII-LNT. A.** Combined Fourier transform from 1000 helical segments. The first and second layer line are centered at 1/82 $Å^{-1}$ and 1/41 $Å^{-1}$ for human FVIII-LNT, and at 1/72 $Å^{-1}$ and 1/36 $Å^{-1}$ for porcine FVIII-LNT (white arrows). **B.** Surface representation of human in pink (Δz =41.1 Å, $\Delta\phi$=42.0º) and porcine in blue (Δz =35.9 Å, $\Delta\phi$=35.2º**)** FVIII-LNT 3D helical reconstructions. Both volumes are presented at 0.005 contour level (minimum density is 0 and maximum density 0.02, as calculated in UCSF Chimera, Volume viewer option [21]). The length of the FVIII-LNT tube is 256 pixels at 2.9 Å/pix. **C.** Fourier Shell Correlation (FSC) plots for human and porcine FVIII-LNT showing a resolution of 20.5 Å at FSC = 0.5.

Figure 5. Helical organization of human and porcine FVIII-LNT. Segmented surface representation of human and porcine FVIII-LNT helical reconstructions, shown in Fig. 4B. The volumes are segmented after imposing 4-fold symmetry to the human FVIII-LNT and 5-fold symmetry to the porcine FVIII-LNT. The asymmetric units are color coded yellow-red for the human FVIII-LNT and blue-green for the porcine FVIII-LNT. **A.** Views along the helical axis indicated with a square for the human and as a pentagon for the porcine FVIII-LNT. The human FVIII-LNT structure shows 8 molecules organized around the outer LNT membrane and the porcine FVIII structure shows 10 molecules organized around the outer LNT membrane, indicated with numbers. **B.** Views perpendicular to the helical axis. The human FVIII-LNT is a 4-start helical structure and the porcine FVIII-LNT is a 5-start helical structure. The individual one start helices are indicated with numbers and color-coded. We have emphasized one of the helices from each structure with a (*) and green lines. The scale bar is 20 nm.

Figure 6. Comparison between the helical and tomography 3D reconstructions. The human FVIII-LNT (**A**) and porcine FVIII-LNT (**C**) helical 3D reconstructions are

shown perpendicular to the helical axis. Each unit cell and individual helices are color-coded as in Fig. 5. **B**. and **D**. are density representations of the 3D tomography reconstructions, viewed perpendicular to the helical axis. The 2D lattice reflecting the helical arrangement of the FVIII molecules is shown with green lines.

DISCUSSION

In this work a methodology is presented to differentiate between two membrane-bound organizations of highly homologous proteins: human and porcine FVIII self-assembled on lipid nanotubes in the conditions encountered in the human body.

In the described procedure, human and porcine FVIII are successfully organized helically on lipid nanotubes, which is the most critical step. The next critical step is to preserve the sample in thin amorphous ice by flash freezing at near liquid N_2 temperature. Preserving the sample in amorphous ice and LN2 temperature keeps the helical tubes hydrated and the protein-lipid macromolecular assemblies physiologically active. The final critical step is acquiring Cryo-EM data of sufficient quantity and quality for a high-resolution 3D structure at near LN2 temperature. Collecting data at near LN2 temperature further prevents dehydration of the sample in the high vacuum of the microscope and radiation damage from the electron beam.

To calculate the membrane-bound structure of the FVIII the first critical step is to obtain homogenous particles (helical segments) sets by applying 2D reference free classification and combine particles from classes with the same diameter and degree of order. The second critical step is to impose the right initial volume and helical parameters (rise and azymuthal angle) for the helical reconstruction. The third and final critical step is to validate the helical structure by comparing the 3D maps obtained by the helical and electron tomography (without imposed symmetry) reconstructions of the same specimen.

The presented methodology is unique in its capacity to resolve the functional structure of membrane associated proteins at near physiological conditions. The LNT developed in our laboratory can be successfully used as a platform for helical organization of functional membrane-bound blood coagulation factors and achieve better resolution than for FVIII organized in membrane-bound 2D crystals and as single particles. Our goal is to further increase the resolution of our helical reconstructions by improving the homogeneity and quality of the final particle sets. Collecting more Cryo-EM micrographs at better Cryo-EM conditions (Field emission gun, energy filter, DE camera detectors) of FVIII-LNT helical filaments and therefore including larger initial particle sets for the 2D reconstruction will achieve this. Improving the FVIII-LNT helical assembly and 3D reconstruction algorithms will allow us to obtain sub-nanometer and near atomic resolution, which will unambiguously define the membrane-bound organization of this critical for blood coagulation protein.

Organizing helically homologous FVIII forms gives us also the opportunity to characterize how difference in sequence can correlate to differences in structure and function. Resolving the human and porcine FVIII membrane-bound structures by the

methods described in this article can help identify the sequences, which when modified will improve the recombinant FVIII function. This knowledge will have significant clinical implications for drug discovery in both Thrombosis and Hemostasis fields.

DISCLOSURE

The authors declare that they have no competing financial interest and they can be contacted directly regarding any of the procedures published in this manuscript.

ACKNOWLEDGMENTS

This work is supported by a National Scientist Development grant from the American Heart Association: 10SDG3500034 and UTMB-NCB start up funds to SSM. The authors acknowledge the Cryo-EM and Scientific Computing facilities at the Sealy Center for Structural Biology at UTMB (www.scsb.utmb.edu), as well as Drs. Steve Ludtke and Ed Egelman for help with the 2D and 3D helical reconstruction algorithms.

REFERENCES

1. Henderson, R. Realizing the potential of electron cryo-microscopy. *Quarterly Reviews of Biophysics* **37**, 3-13, doi:doi:10.1017/S0033583504003920 (2004).
2. Fujiyoshi, Y. & Unwin, N. Electron crystallography of proteins in membranes. *Current opinion in structural biology* **18**, 587-592, doi:10.1016/j.sbi.2008.07.005 (2008).
3. Toole, J. J. *et al.* Molecular cloning of a cDNA encoding human antihaemophilic factor. *Nature* **312**, 342-347 (1984).
4. Fay, P. J. Factor VIII structure and function. *International journal of hematology* **83**, 103-108, doi:10.1532/IJH97.05113 (2006).
5. Stoilova-McPhie, S., Lynch, G. C., Ludtke, S. J. & Pettitt, B. M. Domain organization of membrane-bound factor VIII. *Biopolymers*, In Press, doi:10.1002/bip.22199 (2013).
6. Pipe, S. W. Hemophilia: new protein therapeutics. *Hematology / the Education Program of the American Society of Hematology. American Society of Hematology. Education Program* **2010**, 203-209, doi:10.1182/asheducation-2010.1.203 (2010).
7. Gatti, L. & Mannucci, P. M. Use of porcine factor VIII in the management of seventeen patients with factor VIII antibodies. *Thrombosis and haemostasis* **51**, 379-384 (1984).
8. Parmenter, C. D., Cane, M. C., Zhang, R. & Stoilova-McPhie, S. Cryo-electron microscopy of coagulation Factor VIII bound to lipid nanotubes. *Biochemical and biophysical research communications* **366**, 288-293, doi:10.1016/j.bbrc.2007.11.072 (2008).
9. Parmenter, C. D. & Stoilova-McPhie, S. Binding of recombinant human coagulation factor VIII to lipid nanotubes. *FEBS letters* **582**, 1657-1660, doi:10.1016/j.febslet.2008.04.018 (2008).
10. Wassermann, G. E., Olivera-Severo, D., Uberti, A. F. & Carlini, C. R. Helicobacter pylori urease activates blood platelets through a lipoxygenase-mediated pathway. *Journal of cellular and molecular medicine* **14**, 2025-2034, doi:10.1111/j.1582-4934.2009.00901.x (2010).

11. Wilson-Kubalek, E. M., Chappie, J. S. & Arthur, C. P. Helical crystallization of soluble and membrane binding proteins. *Methods in enzymology* **481**, 45-62, doi:10.1016/S0076-6879(10)81002-X (2010).
12. Egelman, E. H. Reconstruction of helical filaments and tubes. *Methods in enzymology* **482**, 167-183, doi:10.1016/S0076-6879(10)82006-3 (2010).
13. Lusher, J. M. Development and introduction of recombinant factor VIII--a clinician's experience. *Haemophilia : the official journal of the World Federation of Hemophilia* **18**, 483-486, doi:10.1111/j.1365-2516.2012.02804.x (2012).
14. Thim, L. *et al.* Purification and characterization of a new recombinant factor VIII (N8). *Haemophilia : the official journal of the World Federation of Hemophilia* **16**, 349-359, doi:10.1111/j.1365-2516.2009.02135.x (2010).
15. Doering, C. B., Healey, J. F., Parker, E. T., Barrow, R. T. & Lollar, P. High level expression of recombinant porcine coagulation factor VIII. *The Journal of biological chemistry* **277**, 38345-38349, doi:10.1074/jbc.M206959200 (2002).
16. Tang, G. *et al.* EMAN2: an extensible image processing suite for electron microscopy. *Journal of structural biology* **157**, 38-46, doi:10.1016/j.jsb.2006.05.009 (2007).
17. Egelman, E. H. A robust algorithm for the reconstruction of helical filaments using single-particle methods. *Ultramicroscopy* **85**, 225-234 (2000).
18. Egelman, E. H. The iterative helical real space reconstruction method: surmounting the problems posed by real polymers. *Journal of structural biology* **157**, 83-94, doi:10.1016/j.jsb.2006.05.015 (2007).
19. Mastronarde, D. N. Automated electron microscope tomography using robust prediction of specimen movements. *Journal of structural biology* **152**, 36-51 (2005).
20. Stoilova-McPhie, S., Villoutreix, B. O., Mertens, K., Kemball-Cook, G. & Holzenburg, A. 3-Dimensional structure of membrane-bound coagulation factor VIII: modeling of the factor VIII heterodimer within a 3-dimensional density map derived by electron crystallography. *Blood* **99**, 1215-1223 (2002).
21. Goddard, T. D., Huang, C. C. & Ferrin, T. E. Visualizing density maps with UCSF Chimera. *Journal of structural biology* **157**, 281-287, doi:10.1016/j.jsb.2006.06.010 (2007).

*Figure1
Click here to download high resolution image

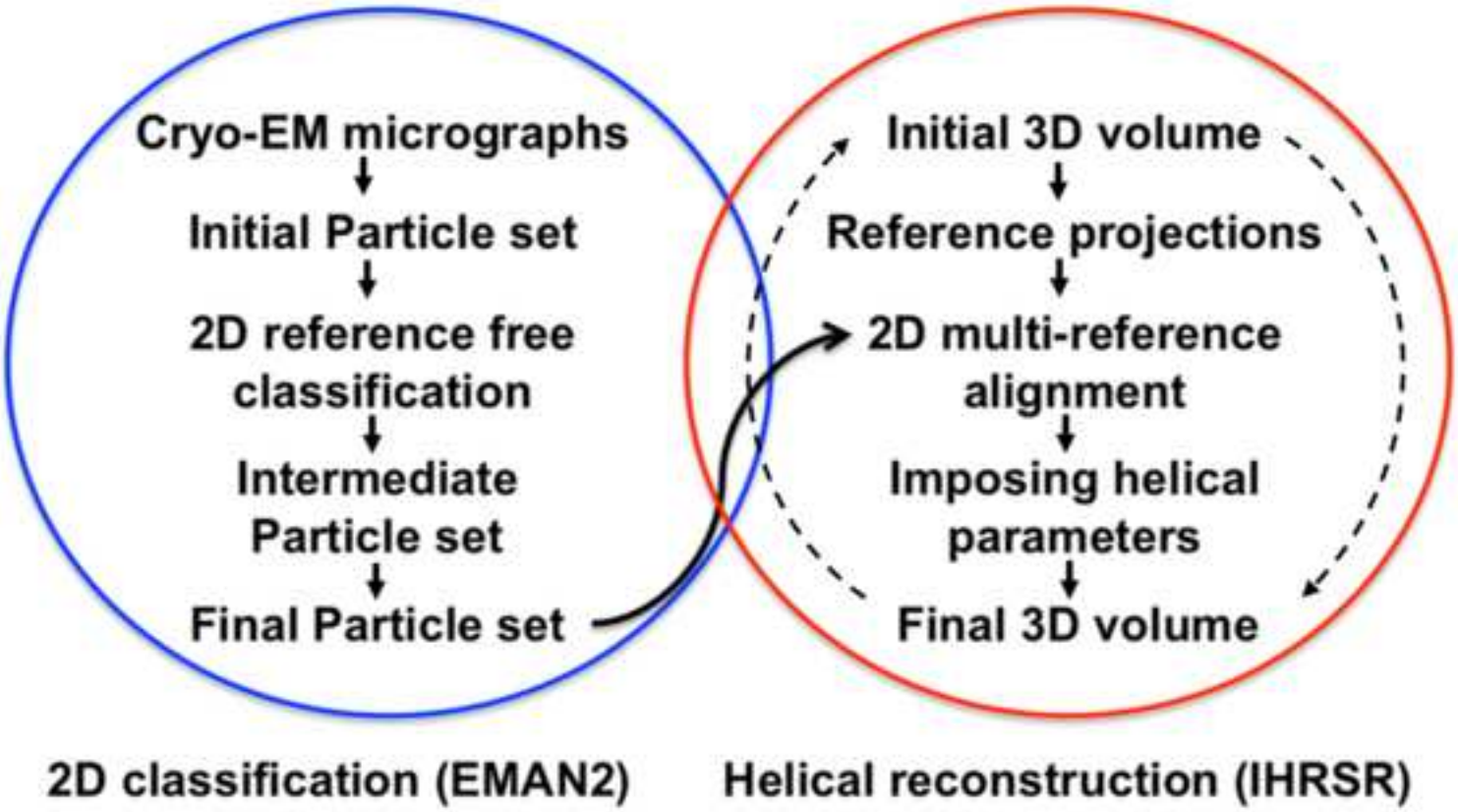

*Figure2
Click here to download high resolution image

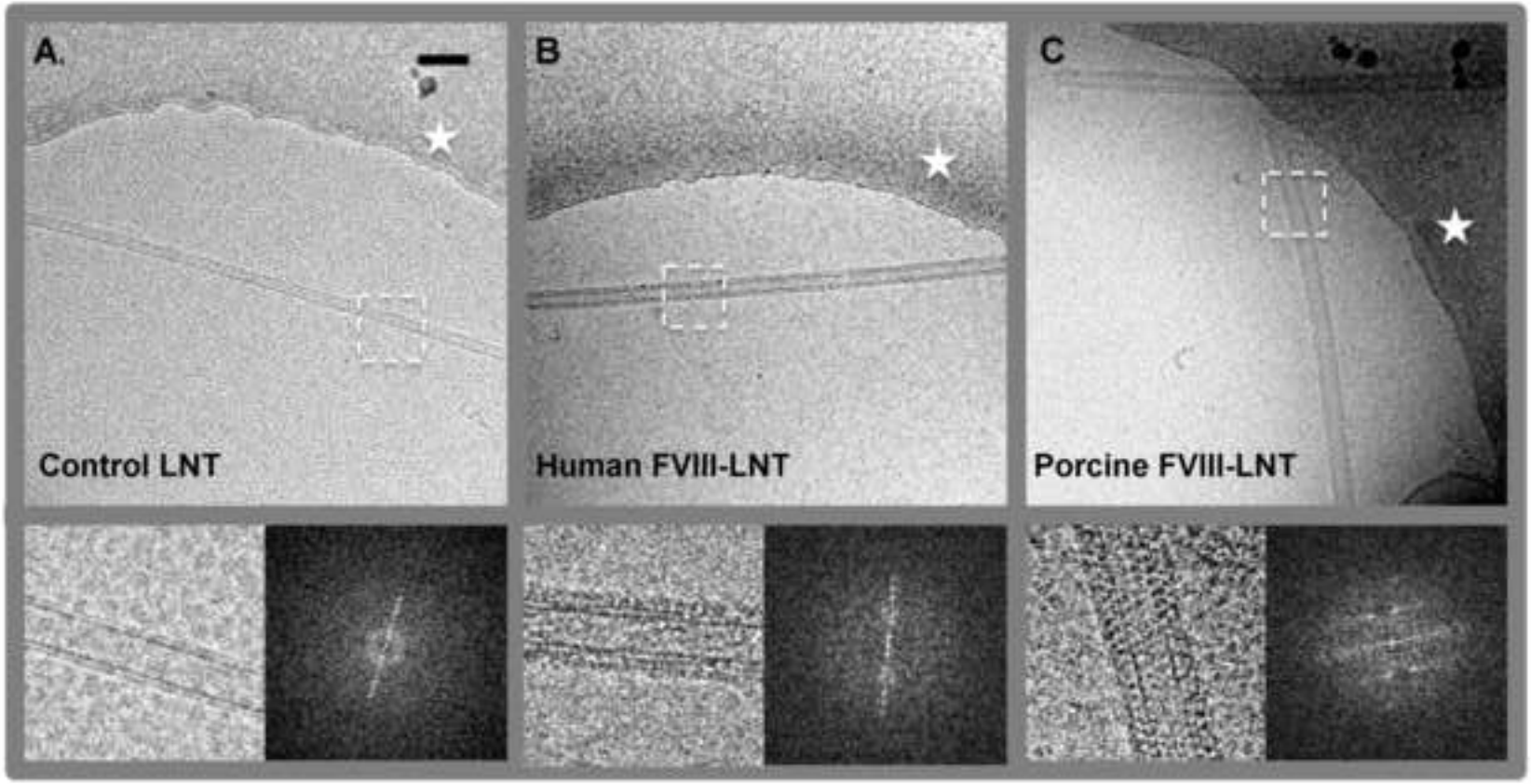

*Figure3
Click here to download high resolution image

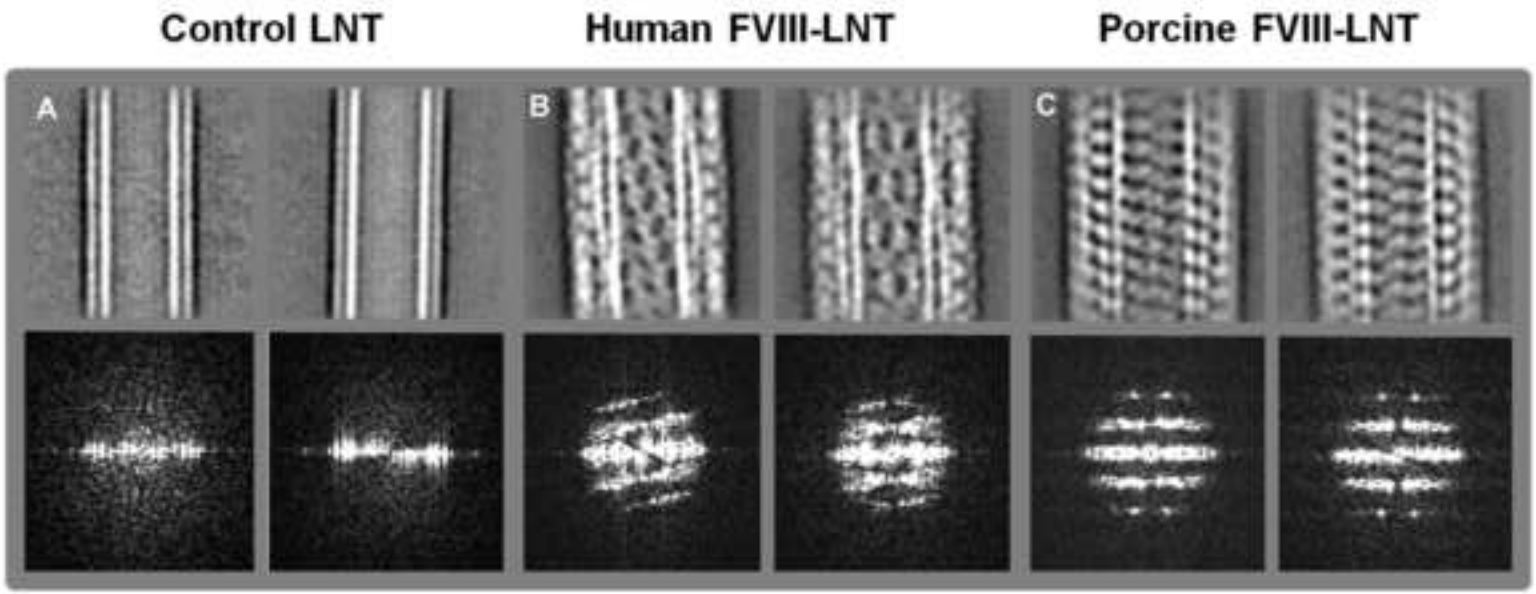

Cass #	48	28	25	16	4	24
Particles #	517	648	734	413	776	484

*Figure4
Click here to download high resolution image

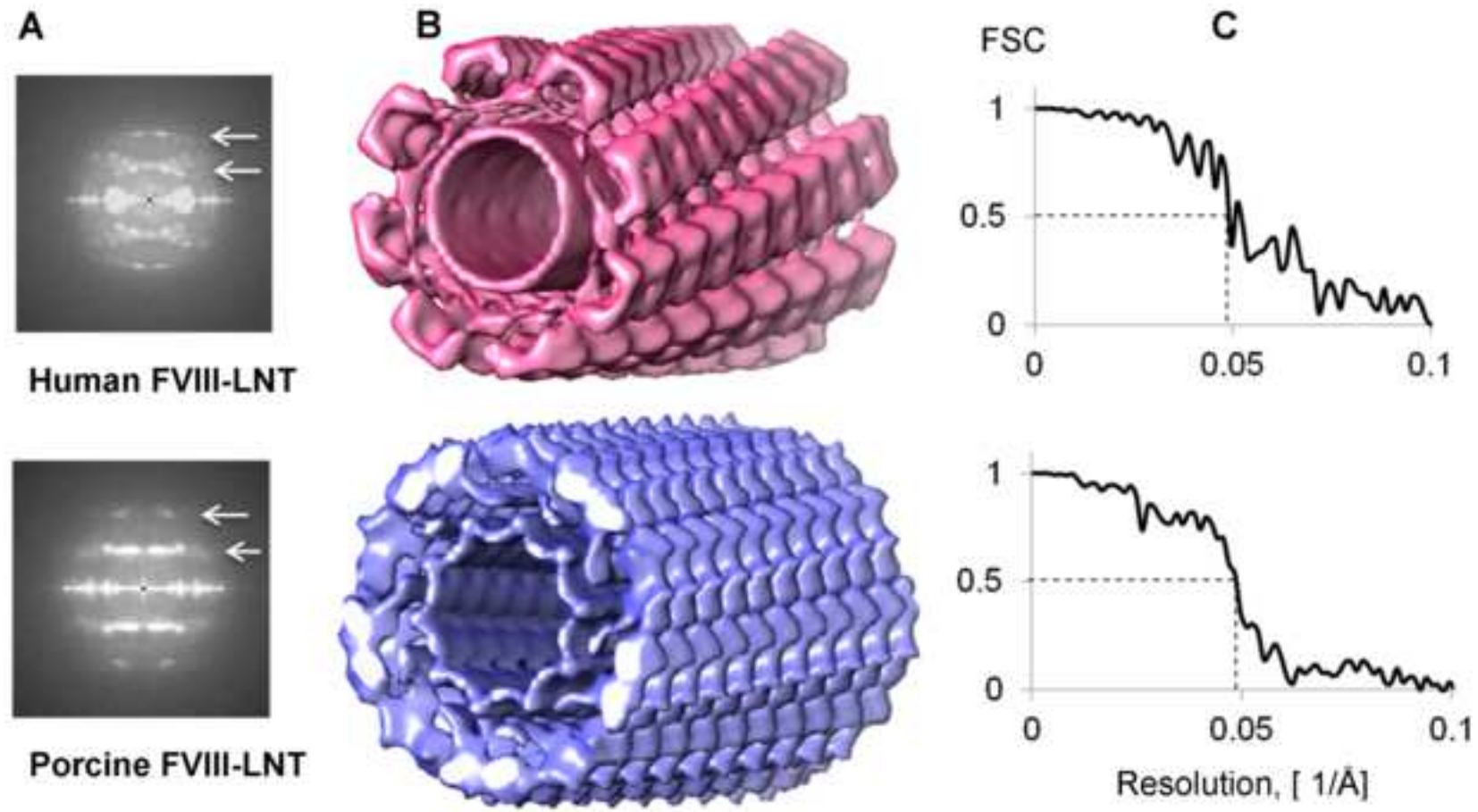

*Figure5
Click here to download high resolution image

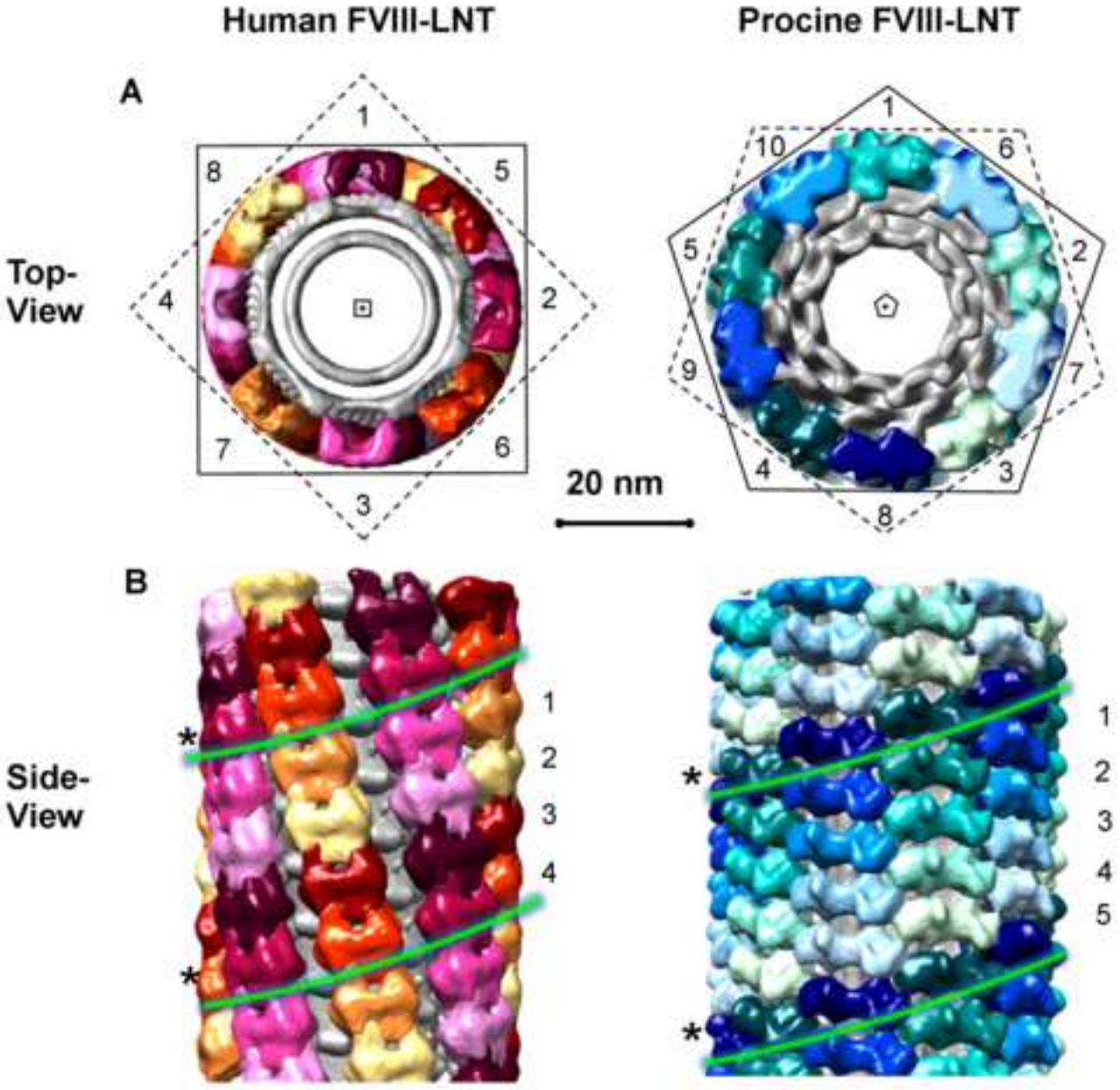

*Figure6
Click here to download high resolution image

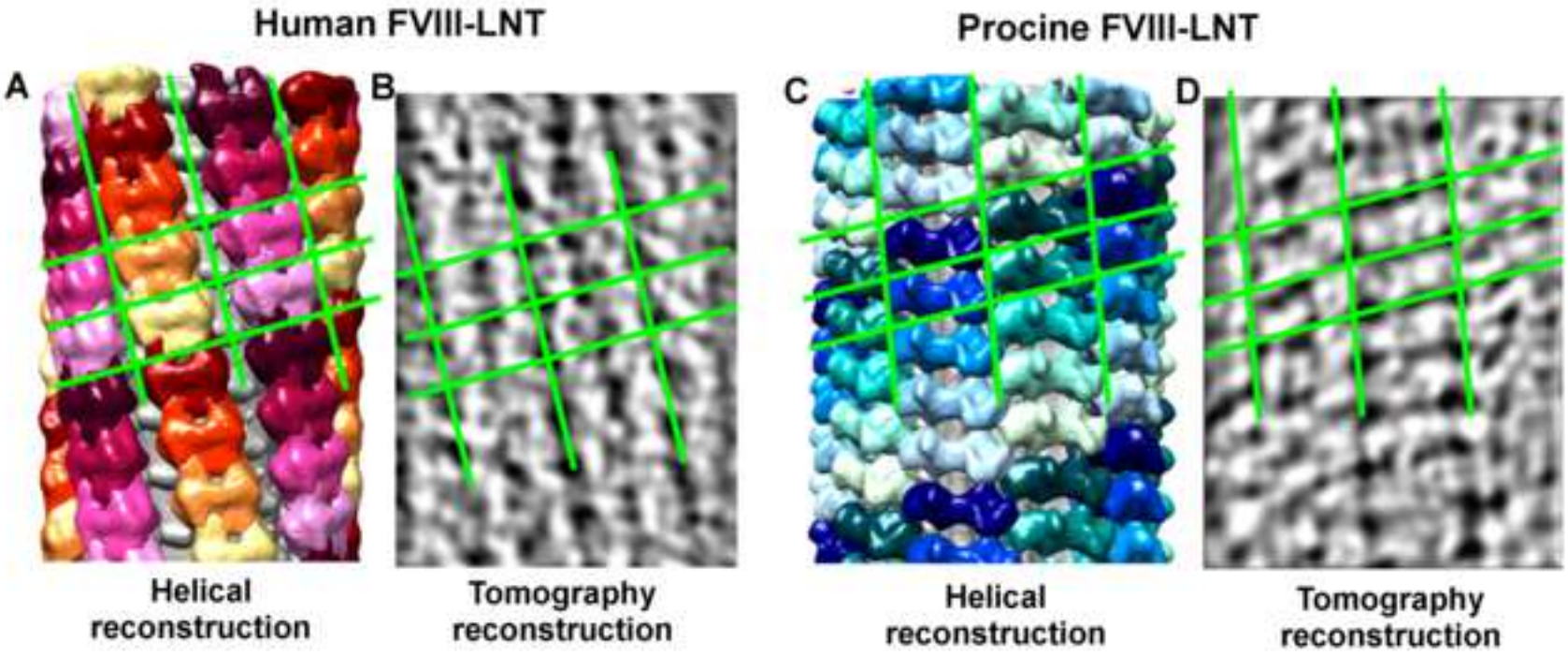

Table1
Click here to download Table: Table1.docx

Table 1.

SAMPLES	cLNT	hFVIII-LNT	pFVIII-LNT
Initial micrographs	61	474	542
Initial Particle sets	29113	60395	64665
Defocus (nm)	-4051 ± 502	-3643 ± 737	-3443 ± 1086
Intermediate Particle sets	25,907	27,305	22,773
Final Particle sets	25,907	10,455	10,430

TABLE 1. 2D analysis statistics following the algorithm presented in the flowchart on Fig. 3.

*Excel Spreadsheet- Table of Materials/Equipment

Click here to download Excel Spreadsheet- Table of Materials/Equipment: JoVE Table of Materials-new.xls

Name of Reagent/ Equipment	Company	Catalog Number
Instruments		
JEM2100 with LaB_6	JEOL Ltd.	JEM-2100
with TEMCON software	JEOL Ltd.	
Gatan626 Cryo-holder	Gatan, Inc.	626.DH
with temperature controler unit	Gatan, Inc.	
Gatan 4K x 4K CCD camera	Gatan, Inc.	US4000
Solarus Model 950 plasma cleaner	Gatan, Inc.	
Vitrobot Mark IV	FEI	
Materials		
Carbon coated 300 mesh 3mm copper grid	Ted Pella	01821
Quantifoil R2/2 300 mesh	Electron Microscopy Sciences	Q225-CR2
Uranyl acetate dihydrate	Ted Pella	19481
Galactosyl ceramide	Avanti Polar Lipids Inc.	860546
Dioleoyl-*sn* -glycero-phospho-L-serine	Avanti Polar Lipids Inc.	840035
Software		
EM software Digital Micrograph	Gatan, Inc.	
EM software EMAN	free download	
EM software Spider	free download	
EM software IHRSR	free download	
EM software (IMOD)	free download	
EM software (SerialEM)	free download	
UCSF-Chimera	free download	

Comments/Description

operated at 200 kV

cooled to -175 °C

4096 x 4096 pixel at 15 microns/pixel physical resolution

plasma cleaned for 10 s on high power
Carbon coated 300 mesh Cu grids with 2 μm in diameters holes
1% solution, filtered

http://www.gatan.com/DM/

http://blake.bcm.edu/emanwiki/EMAN/

http://spider.wadsworth.org/spider_doc/spider/docs/spider.html
Programs available from Edward H. Egelman
http://people.virginia.edu/~ehe2n/
http://bio3d.colorado.edu/imod/
ftp://bio3d.colorado.edu/pub/SerialEM/
http://www.cgl.ucsf.edu/chimera/download.html

17 Sellers Street
Cambridge, MA 02139
tel. +1.617.945.9051
www.JoVE.com

ARTICLE AND VIDEO LICENSE AGREEMENT

Title of Article: Helical organization of blood coagulation factor VIII

Author(s): Sveta Stoilova-McPhie, PhD

Item 1 (check one box): The Author elects to have the Materials be made available (as described at http://www.jove.com/publish) via: ☑ Standard Access ☐ Open Access

Item 2 (check one box):

☑ The Author is NOT a United States government employee.

☐ The Author is a United States government employee and the Materials were prepared in the course of his or her duties as a United States government employee.

☐ The Author is a United States government employee but the Materials were NOT prepared in the course of his or her duties as a United States government employee.

ARTICLE AND VIDEO LICENSE AGREEMENT

1. Defined Terms. As used in this Article and Video License Agreement, the following terms shall have the following meanings: "**Agreement**" means this Article and Video License Agreement; "**Article**" means the article specified on the last page of this Agreement, including any associated materials such as texts, figures, tables, artwork, abstracts, or summaries contained therein; "**Author**" means the author who is a signatory to this Agreement; "**Collective Work**" means a work, such as a periodical issue, anthology or encyclopedia, in which the Materials in their entirety in unmodified form, along with a number of other contributions, constituting separate and independent works in themselves, are assembled into a collective whole; "**CRC License**" means the Creative Commons Attribution-Non Commercial-No Derivs 3.0 Unported Agreement, the terms and conditions of which can be found at: http://creativecommons.org/licenses/by-nc-nd/3.0/legalcode; "**Derivative Work**" means a work based upon the Materials or upon the Materials and other pre-existing works, such as a translation, musical arrangement, dramatization, fictionalization, motion picture version, sound recording, art reproduction, abridgment, condensation, or any other form in which the Materials may be recast, transformed, or adapted; "**Institution**" means the institution, listed on the last page of this Agreement, by which the Author was employed at the time of the creation of the Materials; "**JoVE**" means MyJove Corporation, a Massachusetts corporation and the publisher of *The Journal of Visualized Experiments;* "**Materials**" means the Article and / or the Video; "**Parties**" means the Author and JoVE; "**Video**" means any video(s) made by the Author, alone or in conjunction with any other parties, or by JoVE or its affiliates or agents, individually or in collaboration with the Author or any other parties, incorporating all or any portion of the Article, and in which the Author may or may not appear.

2. Background. The Author, who is the author of the Article, in order to ensure the dissemination and protection of the Article, desires to have the JoVE publish the Article and create and transmit videos based on the Article. In furtherance of such goals, the Parties desire to memorialize in this Agreement the respective rights of each Party in and to the Article and the Video.

3. Grant of Rights in Article. In consideration of JoVE agreeing to publish the Article, the Author hereby grants to JoVE, subject to **Sections 4** and **7** below, the exclusive, royalty-free, perpetual (for the full term of copyright in the Article, including any extensions thereto) license (a) to publish, reproduce, distribute, display and store the Article in all forms, formats and media whether now known or hereafter developed (including without limitation in print, digital and electronic form) throughout the world, (b) to translate the Article into other languages, create adaptations, summaries or extracts of the Article or other Derivative Works (including, without limitation, the Video) or Collective Works based on all or any portion of the Article and exercise all of the rights set forth in (a) above in such translations, adaptations, summaries, extracts, Derivative Works or Collective Works and (c) to license others to do any or all of the above. The foregoing rights may be exercised in all media and formats, whether now known or hereafter devised, and include the right to make such modifications as are technically necessary to exercise the rights in other media and formats. If the "Open Access" box has been checked in **Item 1** above, JoVE and the Author hereby grant to the public all such rights in the Article as provided in, but subject to all limitations and requirements set forth in, the CRC License.

4. Retention of Rights in Article. Notwithstanding the exclusive license granted to JoVE in **Section 3** above, the

Author shall, with respect to the Article, retain the non-exclusive right to use all or part of the Article for the non-commercial purpose of giving lectures, presentations or teaching classes, and to post a copy of the Article on the Institution's website or the Author's personal website, in each case provided that a link to the Article on the JoVE website is provided and notice of JoVE's copyright in the Article is included. All non-copyright intellectual property rights in and to the Article, such as patent rights, shall remain with the Author.

5. Grant of Rights in Video – Standard Access. This **Section 5** applies if the "Standard Access" box has been checked in **Item 1** above or if no box has been checked in **Item 1** above. In consideration of JoVE agreeing to produce, display or otherwise assist with the Video, the Author hereby acknowledges and agrees that, Subject to **Section 7** below, JoVE is and shall be the sole and exclusive owner of all rights of any nature, including, without limitation, all copyrights, in and to the Video. To the extent that, by law, the Author is deemed, now or at any time in the future, to have any rights of any nature in or to the Video, the Author hereby disclaims all such rights and transfers all such rights to JoVE.

6. Grant of Rights in Video – Open Access. This **Section 6** applies only if the "Open Access" box has been checked in **Item 1** above. In consideration of JoVE agreeing to produce, display or otherwise assist with the Video, the Author hereby grants to JoVE, subject to **Section 7** below, the exclusive, royalty-free, perpetual (for the full term of copyright in the Article, including any extensions thereto) license (a) to publish, reproduce, distribute, display and store the Video in all forms, formats and media whether now known or hereafter developed (including without limitation in print, digital and electronic form) throughout the world, (b) to translate the Video into other languages, create adaptations, summaries or extracts of the Video or other Derivative Works or Collective Works based on all or any portion of the Video and exercise all of the rights set forth in (a) above in such translations, adaptations, summaries, extracts, Derivative Works or Collective Works and (c) to license others to do any or all of the above. The foregoing rights may be exercised in all media and formats, whether now known or hereafter devised, and include the right to make such modifications as are technically necessary to exercise the rights in other media and formats. For any Video to which this Section 6 is applicable, JoVE and the Author hereby grant to the public all such rights in the Video as provided in, but subject to all limitations and requirements set forth in, the CRC License.

7. Government Employees. If the Author is a United States government employee and the Article was prepared in the course of his or her duties as a United States government employee, as indicated in **Item 2** above, and any of the licenses or grants granted by the Author hereunder exceed the scope of the 17 U.S.C. 403, then the rights granted hereunder shall be limited to the maximum rights permitted under such statute. In such case, all provisions contained herein that are not in conflict with such statute shall remain in full force and effect, and all provisions contained herein that do so conflict shall be deemed to be amended so as to provide to JoVE the maximum rights permissible within such statute.

8. Likeness, Privacy, Personality. The Author hereby grants JoVE the right to use the Author's name, voice, likeness, picture, photograph, image, biography and performance in any way, commercial or otherwise, in connection with the Materials and the sale, promotion and distribution thereof. The Author hereby waives any and all rights he or she may have, relating to his or her appearance in the Video or otherwise relating to the Materials, under all applicable privacy, likeness, personality or similar laws.

9. Author Warranties. The Author represents and warrants that the Article is original, that it has not been published, that the copyright interest is owned by the Author (or, if more than one author is listed at the beginning of this Agreement, by such authors collectively) and has not been assigned, licensed, or otherwise transferred to any other party. The Author represents and warrants that the author(s) listed at the top of this Agreement are the only authors of the Materials. If more than one author is listed at the top of this Agreement and if any such author has not entered into a separate Article and Video License Agreement with JoVE relating to the Materials, the Author represents and warrants that the Author has been authorized by each of the other such authors to execute this Agreement on his or her behalf and to bind him or her with respect to the terms of this Agreement as if each of them had been a party hereto as an Author. The Author warrants that the use, reproduction, distribution, public or private performance or display, and/or modification of all or any portion of the Materials does not and will not violate, infringe and/or misappropriate the patent, trademark, intellectual property or other rights of any third party. The Author represents and warrants that it has and will continue to comply with all government, institutional and other regulations, including, without limitation all institutional, laboratory, hospital, ethical, human and animal treatment, privacy, and all other rules, regulations, laws, procedures or guidelines, applicable to the Materials, and that all research involving human and animal subjects has been approved by the Author's relevant institutional review board.

10. JoVE Discretion. If the Author requests the assistance of JoVE in producing the Video in the Author's facility, the Author shall ensure that the presence of JoVE employees, agents or independent contractors is in accordance with the relevant regulations of the Author's institution. If more than one author is listed at the beginning of this Agreement, JoVE may, in its sole discretion, elect not take any action with respect to the Article until such time as it has received complete, executed Article and Video License Agreements from each such author. JoVE reserves the right, in its absolute and sole discretion and without giving any reason therefore, to accept or decline any work submitted to JoVE. JoVE and its employees, agents and independent contractors shall have full, unfettered access to the facilities of the Author or of the Author's institution as necessary to make the Video, whether actually published or not. JoVE has sole discretion as to the method of making and publishing the Materials, including,

17 Sellers Street
Cambridge, MA 02139
tel. +1.617.945.9051
www.JoVE.com

ARTICLE AND VIDEO LICENSE AGREEMENT

without limitation, to all decisions regarding editing, lighting, filming, timing of publication, if any, length, quality, content and the like.

11. Indemnification. The Author agrees to indemnify JoVE and/or its successors and assigns from and against any and all claims, costs, and expenses, including attorney's fees, arising out of any breach of any warranty or other representations contained herein. The Author further agrees to indemnify and hold harmless JoVE from and against any and all claims, costs, and expenses, including attorney's fees, resulting from the breach by the Author of any representation or warranty contained herein or from allegations or instances of violation of intellectual property rights, damage to the Author's or the Author's institution's facilities, fraud, libel, defamation, research, equipment, experiments, property damage, personal injury, violations of institutional, laboratory, hospital, ethical, human and animal treatment, privacy or other rules, regulations, laws, procedures or guidelines, liabilities and other losses or damages related in any way to the submission of work to JoVE, making of videos by JoVE, or publication in *JoVE* or elsewhere by JoVE. The Author shall be responsible for, and shall hold JoVE harmless from, damages caused by lack of sterilization, lack of cleanliness or by contamination due to the making of a video by JoVE its employees, agents or independent contractors. All sterilization, cleanliness or decontamination procedures shall be solely the responsibility of the Author and shall be undertaken at the Author's expense. All indemnifications provided herein shall include JoVE's attorney's fees and costs related to said losses or damages. Such indemnification and holding harmless shall include such losses or damages incurred by, or in connection with, acts or omissions of JoVE, its employees, agents or independent contractors.

12. Fees. To cover the cost incurred for publication, JoVE must receive payment before production and publication the Materials. Payment is due in 21 days of invoice. Should the Materials not be published due to an editorial or production decision, these funds will be returned to the Author. Withdrawal by the Author of any submitted Materials after final peer review approval will result in a US$1,200 fee to cover pre-production expenses incurred by JoVE. If payment is not received by the completion of filming, production and publication of the Materials will be suspended until payment is received.

13. Transfer, Governing Law. This Agreement may be assigned by JoVE and shall inure to the benefits of any of JoVE's successors and assignees. This Agreement shall be governed and construed by the internal laws of the Commonwealth of Massachusetts without giving effect to any conflict of law provision thereunder. This Agreement may be executed in counterparts, each of which shall be deemed an original, but all of which together shall be deemed to me one and the same agreement. A signed copy of this Agreement delivered by facsimile, e-mail or other means of electronic transmission shall be deemed to have the same legal effect as delivery of an original signed copy of this Agreement.

A signed copy of this document must be sent with all new submissions. Only one Agreement required per submission.

AUTHOR:

Name: Svetla Stoilova-McPhie

Department: Neuroscience and Cell Biology

Institution: University of Texas Medical Branch

Article Title: Helical organization of blood coagulation Factor VIII on lipid nanotubes

Signature: S McPhie Date: 9/24/2013

Please submit a signed and dated copy of this license by one of the following three methods:

1) Upload a scanned copy as a PDF to the *JoVE* submission site upon manuscript submission (preferred);
2) Fax the document to +1.866.381.2236; or
3) Mail the document to *JoVE* / Attn: *JoVE* Editorial / 17 Sellers St / Cambridge, MA 02139

For questions, please email editorial@jove.com or call +1.617.945.9051.

MS # (internal use):

*Rebuttal Comments
Click here to download Rebuttal Comments: AnswerstoReviewersComments.doc

utmb Health

SCHOOL OF MEDICINE

DEPARTMENT OF NEUROSCIENCE AND CELL BIOLOGY

To the Editor of JoVE November 4th, 2013

I would like to thank the Reviewers for their comments and critiques.

Answers to Reviewer 1:

1. *The manuscript would benefit (e.g. in Figure 1 and in text) to discriminate between regular EMAN single particle software and the more specialized IHRSR software, and explain in a little more detail the differences between them.*

   Figure 1 has been modified by adding plain arrows showing the sequential steps in the 2D and 3D reconstruction panels (circles).
   Figure 1 legend has been also modified explaining the similarity and differences between the two software.
   We have re-written the NOTE paragraph (line 128-145) page 5 to diferenciate between the two software and explain the specificity and availability of the IHRSR software.

2. *Figure 2 would benefit from adjusting image contrast, while clearly cryo-EM is low contrast to begin with, an attempt to show the available information at an optimized contrast (appropriate histogram) would be beneficial. Simple labeling of which panel represents what would be very helpful.*

   We have corrected Figure 2 by increasing the contrast, indicating the zoomed in areas. We have corrected the Figure 2 legend accordingly, emphasizing that these are original digital micrograph with the contrast actually observed on the collected Cryo-EM data. Comparing Fig. 2 and Fig. 3 shows the advantages of 2D class averages over single images in increasing the contrast of the structures we study.

3. *Likewise Fig 3 would benefit from some labeling.*

   Figure 3 and legend have been corrected accordingly.

4. *Figure 4 should feature a Fourier Shell Correlation figure to determine the resolution of each reconstruction.. Also the FSC should be discussed in text.*

   The Fourier Shell correlation has been added to Figure 4. The procedure has been described in the text under PROTOCOL section 3.2.5 (p.6:220-222).

5. *Fig 5 and 6 would benefit from some direct labeling of the panels.*

   We have added direct labeling to Figures 5 and 6.

6. *Table of Materials/Equipment should pay attention to layout possible be a table with clear delineation of different fields, as currently not all columns are well aligned*.

   We have delineated clearly the different fields in the Table of Materials/Equipment.

5.212D BUILDING 17, 301 UNIVERSITY BOULEVARD GALVESTON, TEXAS 77555-0620
Cell : 979-319-1349, Office : (409) 747-2203, Fax : (409) 747-2200,
Email: svmcphie@utmb.edu, Web: http://svetla-mcphie-cryoem.com/

Answers to reviewer 2.

1. *Minor Concerns:*
   Minor typos and corrections:
   line 34: The abbreviation "LNT" is used without first being defined.
   line 53: The abbreviation "PS" is not defined.
   line 82: "Buffers exchange purified human..." is confusing and ambiguous.
   line 91: Is the ratio of O2 to He important?
   line 100: Perhaps include an instruction to evacuate the dewar before cooling, and equilibrate after adding N2?
   lines 103-126: Are the function keys referred to (F6,F2,F4,F3) the default keys for the MDS?
   line 113: what is the target defocus?
   line 126: How should the quality and defocus be checked? Does ctrl-F produce an FFT?
   line 140: typo "inverteded" should be "inverted"
   line 208: Does the tomogram need to be aligned, or does SerialEM record images that are already well-aligned?
   line 299: typo "procine" should be "porcine".

   All minor concerns have been addresses and typos have been corrected.

Answers to reviewer 2.

1. *There are several typographical errors within this manuscript, which are distracting. For example, line 82 states, "buffers exchange". This does not make grammatical sense, and there are several instances of this sort throughout the body of the manuscript.*

   The typographical errors through the manuscript have been corrected. We have also looked for logical and grammatical inconsistence and corrected accordingly

2. *The more significant concern about this manuscript is the lack of experimental detail and rationale for why certain aspects are being performed.*

   We have clarified in the text the rationale for the performed experiments described in the ABSTRACT section (p2: 30-43) by modifying a sentence in the INTRODUCTION section (p. 3:59-61). Logical inconsistencies has been corrected through the text in the PROTOCL, REPRESENTATIVE RESULTS and DISCUSSION sections to address this critique.

3. *The authors should list clearly which electron microscope and other systems that are used in this study. To illustrate my frustration in reading this manuscript, I read in the protocols to push "F6" multiple times. What is F6, and why would I be pushing it? Why would I want/need to do a multitude of tasks listed in the procedures?*

   The instruments are listed in the Table of Materials/Equipments and we have written this table for clarity. We have clarified the Minimum dose and electron microscope settings on the JEM2100-LaB6 transmission electron microscope used in the described experiments by adding a note in the PROTCOL section (p4: 102-118). Collecting Cryo-EM data as described in the PROTOCL section is still a state-of-the art procedure, which requires expertise and understanding of each step of the PROTOCOL. Missing any of these steps or using the incorrect order makes the difference between good and bad data, which defines the consecutive structure analysis. These steps have to be optimized for different specimens and datasets accordingly. The procedures presented in this paper are required to achieve the representative results discussed in the manuscript.

4. I believe the authors should trade in the concise nature of their protocols for a more exhaustive explanation of each step being taken. This will make this manuscript much more useful for numerous

5.212D BUILDING 17, 301 UNIVERSITY BOULEVARD GALVESTON, TEXAS 77555-0620
Cell : 979-319-1349, Office : (409) 747-2203, Fax : (409) 747-2200,
Email: svmcphie@utmb.edu, Web: http://svetla-mcphie-cryoem.com/

investigators that would be interested in studying peripheral proteins and their interactions with lipid surfaces.
The LNT helical crystallization technique described in the protocol is the one used in our laboratory. We have added the concentrations of our stock protein and lipid solutions in the PROTOCOL section (p3:83-89). These conditions have to be modified and optimized for each lipid-protein system.
The key of a successful LNT assisted helical crystallization of membrane-associated protein is in performing carefully the sample preparation and Cryo-EM experiments. It is a widely empirical approach, similar to 3D crystallization trials, where the only way of achieving the good crystallization and sample preparation conditions is by repeating and improving over and over the same procedure. Our success rate is close to 80% for the proteins shown in this study.

We have added a comment to the DISCOLSURE section that we can be contacted directly for additional details and guidance needed to perform any of the described experiments.

I hope our revision will satisfy the Reviewer's comments and critiques.

Sincerely,

Svetla S. McPhie

Svetla Stoilova-McPhie. PhD
Assistant Professor
Neuroscience and cell Biology
Sealy Centre for Structural Biology and Molecular Biophysics
University of Texas Medical Branch, Galveston, TX, 77555, USA